

Simulation of single-photon state tomography using phase-randomized coherent states

P. Valente and A. Lezama*

*Instituto de Física, Facultad de Ingeniería, Universidad de la República,
J. Herrera y Reissig 565, 11300 Montevideo, Uruguay*

(Dated: January 28, 2023)

We have experimentally simulated the quantum state tomography of single-photon states of temporal modes of duration T and constant amplitude using phase randomized coherent states (PRCS). A stationary laser beam, whose phase relative to a local oscillator is varied at random, was used as a multiple realization of a PRCS of the temporal mode. The quadrature fluctuations histograms corresponding to the marginal distributions of the PRCS, were acquired with an oscilloscope using a sampling period T . Following a recent suggestion by Yuan et al [1], we have derived estimates for the marginal distribution of the single-photon state. Based on these estimates, the approximate Wigner function and density matrix of the single-photon state were reconstructed with good precision. The sensitivity of the simulation to experimental errors and the number of PRCS used is addressed.

PACS numbers: 03.65.Wj, 42.50.Dv, 03.67.Dd

INTRODUCTION

Many quantum information protocols rely on single-photon states [2]. A well known example is quantum key distribution (QKD) [3–5]. However, deterministic single-photon sources are still not readily available [6, 7] and probabilistic single-photon sources, such as heralded parametric down conversion, are inefficient and too complex and expensive to be practical in commercial devices. In consequence, many practical implementations of quantum information protocols use, instead of single-photon pulses, attenuated coherent state pulses that can be produced on demand. However, the use of weak coherent state (WCS) pulses carries its disadvantages. On one hand it is inefficient since most pulses carry no photon and, more importantly, it jeopardizes security since the probability for two or more photons is non-zero which allows for different forms of attack by an eavesdropper [8–12].

The security issue of QKD with WCS has been solved through the decoy state method [5, 13–19]. In essence, Alice, the sender, uses a random set of WCS of different amplitudes. On the receiving end, Bob analyses the received data and is able, after communicating with Alice, to detect the presence of a possible eavesdropper. More specifically, Bob and Alice are able to extract from the information obtained with WCS of different amplitudes, the yield through the communication channel of the single-photon states and compute the amount of information leaked to a possible eavesdropper [13, 19].

In a recent paper, Yuan et al. [1] have introduced a generalization of the decoy state method to the simulation of an arbitrary quantum process relying on single photon-states. In their article, a detailed theoretical analysis is made for a process ending with a binary measurement outcome (“click” or “no-click”).

The fact that coherent states can be used to characterize an arbitrary quantum process has been signalled in the past [20]. However, as far as single-photon states are concerned, it results from [1] that phase randomized coherent states (PRCS) suffice for the process characterization. Moreover, in this case, the estimation of the single-photon yield of the process can be obtained through simple linear algebra.

In this article we present an experimental verification of the results of [1] and their generalization to quantum processes resulting in a continuous variable outcome. Specifically we demonstrate that the quantum tomography of a single-photon state of a temporal mode can be efficiently simulated with a small ensemble of PRCS. The first experiments on quantum tomography of single-photon states were carried by Lvovsky et al [21] using heralded photons from parametric down-conversion.

The temporal modes considered here are of constant amplitude during the finite time interval T ($T = 400$ ns in the experiments described below). A stationary light beam can thus be viewed as many consecutive realizations of the field state in the temporal mode. More precisely, a well stabilized laser beam can be considered to a good approximation as the multiple realization of a coherent state $|\alpha\rangle$. If the phase of the laser beam is varied at random between different realizations of the temporal mode, then the prepared state is a PRCS with mean photon-number $\mu = |\alpha|^2$.

Following the usual quantum tomography sequence [22], we have initially determined an approximation to the field quadrature probability density (marginal distribution) of the single photon state. For this, the marginal distributions of several PRCS were acquired and combined according to [1] to derive an approximation to the marginal distribution of the single-photon state. In a sec-

ond time, the approximate Wigner function of the single-photon state and the corresponding density matrix was derived. Our example shows that an excellent approximation is obtained even for a reduced number of mean photon-numbers values.

THEORETICAL BACKGROUND

The density matrix for a phase averaged coherent state of mean photon number μ is given by:

$$\rho_\mu = \sum_{k=0}^{\infty} P_\mu(k) |k\rangle\langle k| \quad (1)$$

where $|k\rangle$ designates a Fock state with photon number k and

$$P_\mu(k) = \frac{\mu^k}{k!} e^{-\mu} \quad (2)$$

If a measurement is performed on the system in the state ρ_μ , the probability X_μ for an outcome x is given by:

$$X_\mu(x) = \sum_{k=0}^{\infty} P_\mu(k) P(x|k) \quad (3)$$

where $P(x|k)$ denotes the probability for an outcome x when the system is prepared in the Fock state $|k\rangle$.

Unlike in [1] where expression (3) was applied to a binary measurement with two discrete outcomes (“click” or “no-click”), here we consider a measurement with a continuous variable outcome x . In consequence, $X_\mu(x)$ is the probability density for the measurement outcome to be in the range $[x, x + dx]$. Notice that

$$X_\mu(x), P(x|k) \geq 0 \quad (4a)$$

$$\int X_\mu(x) dx = \int P(x|k) dx = 1 \quad (4b)$$

Following [1], we introduce the notation $Y_k \equiv P(x|k)$. The values of μ and X_μ (we drop the x dependence for compactness) can be experimentally determined. Since X_μ is linearly related to the Y_k 's via Eq. (3), the knowledge of X_μ for a sufficiently large ensemble of values of μ should allow the approximate determination of the single-photon yield Y_k . Following an analysis inspired on the decoy state method of QKD [13], Yuan et al have derived several estimates for Y_1 depending on the available values of the mean-photon-numbers μ [1].

Keeping in mind the Y_k and X_μ refer here to continuous variable distributions, the results derived in [1] concerning the estimate of Y_1 remain valid. They are reminded next.

If only the vacuum and a single value of μ are available, the estimate for Y_1 is:

$$Y_1^{est(1)} = \frac{(X_\mu e^\mu - X_0)}{\mu} \quad (5)$$

which is an upper bound of Y_1 (see Eq. (15) in [1]).

On the other hand, when the information regarding the vacuum state ($\mu = 0$) and two or more values of $\mu \neq 0$ is available the estimate of Y_1 is given by:

$$Y_1^{est(L)} = \sum_{j=0}^L \lambda_j X_{\mu_j} \quad (6)$$

$$\lambda_0 = -\mu_1 \mu_2 \cdots \mu_L \sum_{j=1}^L \frac{\mu_j^{-2}}{\prod_{1 \leq n \leq L, n \neq j} (\mu_n - \mu_j)},$$

$$\lambda_{j \geq 1} = \mu_1 \mu_2 \cdots \mu_L \frac{\mu_j^{-2} e^{\mu_j}}{\prod_{1 \leq n \leq L, n \neq j} (\mu_n - \mu_j)}.$$

This estimate is an upper(lower) bound for Y_1 depending on L being odd(even) [see Eq. (19) in [1]].

In this paper we illustrate the application of expressions (5) and (6) to the determination of the probability density of the field quadrature $\hat{X}_\theta \equiv (ae^{-i\theta} + a^\dagger e^{i\theta})/2$ for the single photon state $|1\rangle$. a and a^\dagger are the usual photon annihilation and creation operators. Since all states considered in this work have no definite phase, the probability distribution of X_θ is independent of θ , we will consequently drop the suffix. Notice that with the above definition the variance of \hat{X} in the vacuum state (or in a coherent state) is $\langle 0|\hat{X}^2|0\rangle = 1/4$.

The expected probability distribution for the outcomes of \hat{X} for a phase averaged coherent state of mean photon-number μ is given by (3) where $P(x|k)$ are the squares of the well known Hermite-Gauss eigenfunctions of the harmonic oscillator with k excitations.

EXPERIMENT

The experimental setup is presented in Fig. 1. The signal and local oscillator (LO) light beams are obtained from the same extended cavity diode laser and separated in an optical fiber beam splitter (FBS). The power in the local oscillator was approximately 10 mW. The signal beam power after the FBS was attenuated to picowatt values using a combination of neutral density filters, half-wave plate and polarizer. The signal beam and the LO are recombined in a beamsplitter in the usual balanced homodyne detection configuration. Detection is achieved with a photodetector pair specifically designed for balanced detection (Thorlabs PDB120A).

The relative phase difference between the signal and the LO optical fields was varied with a mirror mounted

RESULTS AND DISCUSSION

Mean photon number determination

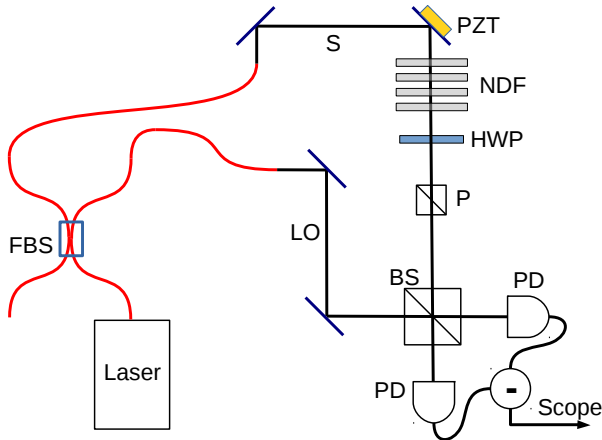


FIG. 1. (Color online) Experimental setup. FBS: fiber beam splitter, BS: beam splitter, PZT: piezo-electric actuator, NDF: neutral density filters, P: polarizer, HWP: half-wave plate, PD: photodetectors, S: signal beam path, LO: local oscillator beam path.

on piezo-electric actuator (PZT). The contrast in the interference fringes between signal and LO is better than 98%. During data acquisition, in order to produce the phase randomization, a triangular voltage ramp is applied to the PZT with an amplitude corresponding to an approximately integer number of 2π phase differences and a frequency near 100 Hz.

The difference of the two photodetector outputs, which is proportional the signal field quadrature, was monitored in a digital oscilloscope (Tektronix DPO4102B, 1 GHz bandwidth, maximum sampling rate: 5 GS/s).

The balanced detector signal was sampled with a sampling frequency of 2.5 MHz. The recorded sample value corresponds to the average over the sampling interval of many scope internal acquisitions taken at the fastest scope sampling rate (High Resolution mode). This ensures that the amplitude of the sampled signal fluctuations scales as the inverse square-root of the interval duration. Each sampling record consisted of 10^7 samples. For each record, the mean value of the fluctuations was subtracted and a histogram of the fluctuations computed. The final histogram was the average over 100 similar sampling records.

With the signal beam blocked, we checked that the variance of the quadrature fluctuations increases linearly with the LO power as expected for vacuum fluctuations.

After acquisition, the experimental histograms were rescaled. From the histogram corresponding to the vacuum state, we computed the sample variance of the fluctuations. This can be achieved with high relative precision (typically 10^{-4}), given the large number of acquired data points. Subsequently, the horizontal axis was rescaled for the vacuum state fluctuations to have a variance equal to $1/4$. The vertical axis scale of each histogram was chosen such that the sum of all the histogram columns multiplied by Δx equals 1 (normalization condition), with Δx being the renormalized distance between two consecutive histogram columns.

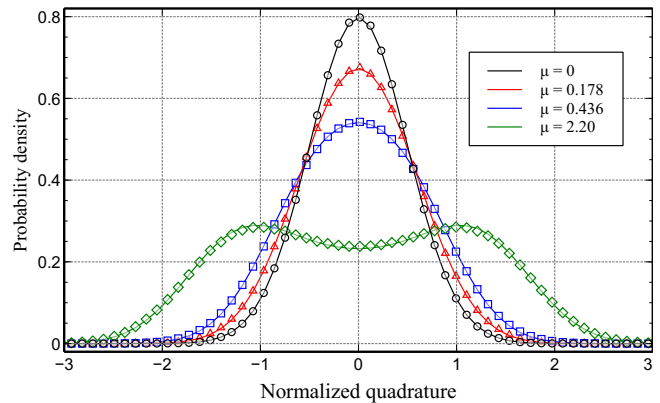


FIG. 2. (Color online) Symbols: Experimental histograms for different mean photon-number values. Solid lines: Calculated $X_\mu(x)$ from Eq. (3) using the values of μ indicated in the figure.

The histograms obtained for the vacuum state and three different signal field intensities are presented in Fig.(2). Notice that the histogram corresponding to the vacuum state is well fitted by a Gaussian distribution. The histograms corresponding to non-zero signal field intensities were fitted to Eq. (3) using μ as an adjustable parameter [23]. The best fits were obtained for $\mu = 0.178 \pm 0.002$, 0.436 ± 0.004 and 2.20 ± 0.01 . The corresponding plots of $X_\mu(x)$ are represented as continuous lines in Fig. (2). Notice the good agreement between the experimental data and the theoretical prediction. While very small, there are some deviations between the recorded histograms and the theoretical distributions given by Eq. (3). These deviations are mainly due to imperfect phase randomization and electronic noise background.

We take the values of μ arising from the fitting procedure described above as the experimental mean photon-number values. We have checked that these values are consistent with the photon-number estimation obtained

from the light power at the optical fiber beamsplitter output and the calibration of the neutral density filters used for attenuation. We have also verified that the mean photon numbers scale linearly with the signal light power and the duration of the sampling interval.

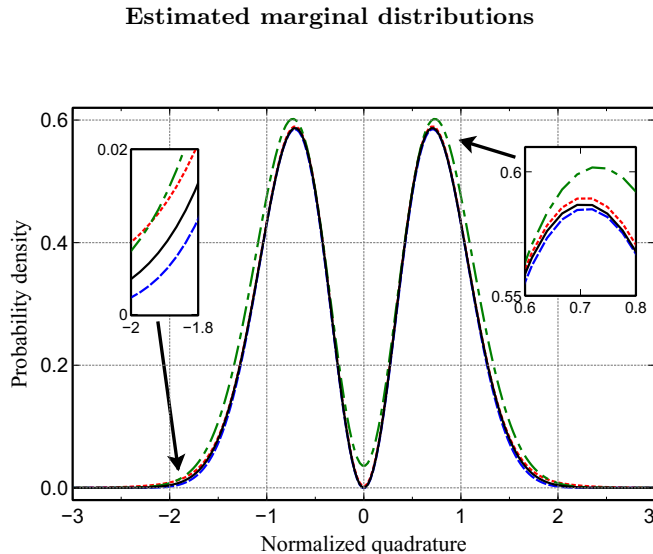


FIG. 3. (Color online) Single photon quadrature probability density distribution. Solid line: exact. Dash-dotted: Estimation according to Eq. (5) using $\mu = 0.178$. Dashed: Estimation according to Eq. (6) using $\mu = 0.178, 0.436$. Dotted: Estimation according to Eq. (6) using $\mu = 0.178, 0.436, 2.20$. For all the estimations de theoretical values of $X_\mu(x)$ given by Eq. (3) were used.

Figure 3 shows the estimates of the single photon quadrature probability distribution obtained with Eq. (5) and (6) from the *theoretical* marginal distributions corresponding to the observed mean-photon numbers. The dashed-dotted line corresponds to the use of Eq. (5) to a single non-zero μ in addition to the vacuum state. The dashed and dotted lines correspond to Eq. (6) applied to the vacuum and two and three non-zero μ 's respectively. As predicted in [1] the estimation for a single non-zero PRCS is an overestimation of the exact probability distribution. Closer approximations are obtained when the number of PRCS's used is increased. Notice that tight upper and lower bounds to single-photon probability distribution are obtained if number of μ 's with different parities are used.

It is worth reminding that the distribution obtained from the application of Eqs. (5) and (6) are not assured to satisfy the requirements in Eqs. (4). These requirements are only met approximately [1].

Figure 4 shows the estimated marginal distributions for the single-photon state computed directly from the experimental histograms of the quadrature fluctuations of

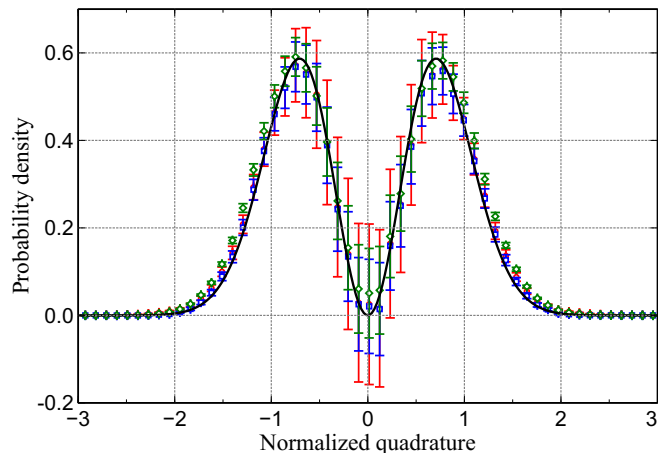


FIG. 4. (Color online) Estimates of the single photon quadrature probability density using the experimental histograms in Fig. (3). Diamonds (green): Estimate using Eq. (5) and $\mu = 0.178$. Squares (blue): Estimate using Eq. (6) and $\mu = 0.178, 0.436$. Circles (red): Estimate using Eq. (6) and $\mu = 0.178, 0.436, 2.20$. Solid line: theoretical value.

the PRCS. As expected, the single-photon marginal distribution is affected by measurement uncertainties. The error bars in Fig. 4 were computed from Eqs. (5) and (6) using standard error propagation formula. While the statistical uncertainties in the histograms play a relatively minor role (in view of the large number of acquired samples) the error bars are mainly determined by the uncertainties in the values of the mean-photon numbers. The largest errors occur near the center of the distribution where the vacuum fluctuations and the fluctuations corresponding to small mean photon numbers are maximum and add-up. Notice the relatively large errorbars in spite of the small ($\sim 10^{-2}$) relative uncertainties of mean-photon numbers.

Wigner function and density matrix reconstruction

In quantum tomography [22] the quantum state Wigner function can be derived from the observed marginal distributions using the inverse Radon transformation. However, because the marginal distribution are affected by experimental error, this method does not ensure that the obtained Wigner function corresponds to a physical state. To circumvent this problem, other techniques such as maximum likelihood or maximum entropy [22] have been suggested. These techniques are suitable for the reconstruction of the density matrix in the present case. However, based on the good agreement between experiment and theoretical expectations for PRCS observed in Fig. (2), we follow a simpler procedure only based in the experimental determination of the PRCS mean-photon numbers. We stress that as a consequence of this simplification, the physical constraints

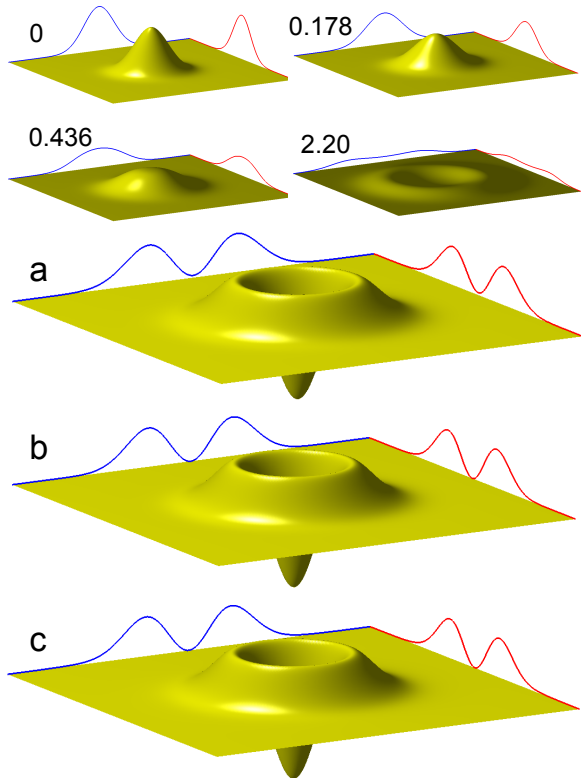


FIG. 5. (Color online) Two upper rows: Calculated Wigner functions and marginal distributions for phase-averaged coherent states with $\mu = 0, 0.178, 0.436$ and 2.20 respectively. Three lower rows: Reconstructed Wigner function and marginal distributions for the single photon state using Eq. (7) with different number of non-zero mean photon numbers. a) Vacuum plus one. b) Vacuum plus two. c) Vacuum plus three. [μ values indicated in first column of Table I]

on the Wigner function and the reconstructed density matrix are relaxed as discussed below.

Since the estimated marginal distribution is a linear combination of the observed marginal distributions for PRCS [Eq. (6)], the corresponding reconstructed Wigner function $W^{est}(r)$ must be linearly related to PRCS's Wigner functions $W_{\mu_j}(r)$ [r is the radial distance to the phase-space origin].

$$W^{est}(r) = \sum_{j=0}^L \lambda_j W_{\mu_j}(r) \quad (7)$$

Figure 5 shows the theoretical Wigner function plots $W_{\mu_j}(r)$ for $\mu = 0, 0.178, 0.436$ and 2.20 and the corresponding reconstructed Wigner functions $W^{est}(r)$ obtained using Eq. (7) for an increasing number of nonzero PRCS (first column in Table I). Even for a single value of $\mu \neq 0$, the similarity to the single-photon Wigner function is striking (see [24]). Better approximations to the exact Wigner function are obtained as

the number of PRCS increases.

In a similar way, the estimated density matrix ρ^{est} (in the Fock states basis) can be calculated as a linear combination of the density matrices ρ_μ corresponding to the phase-averaged coherent states. Notice that by this means ρ^{est} , albeit hermitian, is not assured to possess the usual physical requirements ($\rho > 0$ and $Tr(\rho) = 1$) which are only approximately satisfied.

$\mu \neq 0$	$Tr(\rho^{est})$	$ \rho^{est} - 1\rangle\langle 1 $	Eigenvalues < 0
0.178	1.095	8.9×10^{-2}	No
0.178, 0.436	0.985	1.3×10^{-2}	Yes
0.178, 0.436, 2.20	1.013	8.3×10^{-3}	No

TABLE I. Reconstructed density matrix characteristics for different number of phase-averaged coherent states

In order to quantitatively characterize the quality of the reconstructed density matrix we use the distance $|\rho^{est} - |1\rangle\langle 1||$ between ρ^{est} and the single photon density matrix [we use $|M| \equiv Tr(MM^\dagger)^{1/2}$]. For reference: the distance between two different Fock states is $\sqrt{2}$.

Table I summarizes the characteristics of the reconstructed density matrices for different numbers of phase-randomized coherent states in addition to the vacuum. Notice that as the number of non-zero intensity PRCS increases, $Tr(\rho^{est})$ closely approaches the physical requirement of unity and the distance to the exact single photon density matrix decreases. Also when the number of non-zero intensity PRCS is even, ρ^{est} possesses negative eigenvalues. As clearly shown in Fig. 5 and table I, most of the information required for the single-photon state reconstruction originates from the vacuum and the smallest mean photon number. Additional PRCS with increasing photon-numbers only provide small improvements to the single-photon density matrix reconstruction.

CONCLUSIONS

In summary, we have shown experimentally that PRCS can be simply and efficiently used to simulate the tomography of single-photon temporal states. Similar techniques can be applied to characterize any single photon quantum channel without the requirement of actual single-photon sources.

A.L. is thankful to D. Gauthier for motivating discussions. This work was supported by ANII, CSIC and PEDECIBA (Uruguayan agencies).

* alezama@fing.edu.uy

- [1] X. Yuan, Z. Zhang, N. Lutkenhaus, and X. Ma, “Simulating single photons with realistic photon sources,” <https://arxiv.org/abs/1609.06799>.
- [2] M. A. Nielsen and I. L. Chuang, *Quantum computation and quantum information* (Cambridge university press, 2010).
- [3] H. Bennett Ch and G. Brassard, in *Conf. on Computers, Systems and Signal Processing (Bangalore, India, Dec. 1984)* (1984) pp. 175–9.
- [4] A. K. Ekert, Phys. Rev. Lett. **67**, 661 (1991).
- [5] T. Schmitt-Manderbach, H. Weier, M. Fürst, R. Ursin, F. Tiefenbacher, T. Scheidl, J. Perdigues, Z. Sodnik, C. Kurtsiefer, J. G. Rarity, *et al.*, Physical Review Letters **98**, 010504 (2007).
- [6] B. Lounis and M. Orrit, Reports on Progress in Physics **68**, 1129 (2005).
- [7] Y.-M. He, Y. He, Y.-J. Wei, D. Wu, M. Atatüre, C. Schneider, S. Höfling, M. Kamp, C.-Y. Lu, and J.-W. Pan, Nature nanotechnology **8**, 213 (2013).
- [8] C. H. Bennett, F. Bessette, G. Brassard, L. Salvail, and J. Smolin, Journal of Cryptology **5**, 3 (1992).
- [9] M. Dušek, M. Jahma, and N. Lütkenhaus, Phys. Rev. A **62**, 022306 (2000).
- [10] G. Brassard, N. Lütkenhaus, T. Mor, and B. C. Sanders, Phys. Rev. Lett. **85**, 1330 (2000).
- [11] W.-Y. Hwang, Phys. Rev. Lett. **91**, 057901 (2003).
- [12] D. Gottesman, H. K. Lo, N. Lutkenhaus, and J. Preskill, in *Information Theory, 2004. ISIT 2004. Proceedings. International Symposium on* (2004) pp. 136–.
- [13] H.-K. Lo, X. Ma, and K. Chen, Physical review letters **94**, 230504 (2005).
- [14] X. Ma, B. Qi, Y. Zhao, and H.-K. Lo, Physical Review A **72**, 012326 (2005).
- [15] X.-B. Wang, Phys. Rev. Lett. **94**, 230503 (2005).
- [16] Y. Zhao, B. Qi, X. Ma, H.-K. Lo, and L. Qian, Phys. Rev. Lett. **96**, 070502 (2006).
- [17] H. Inamori, N. Lütkenhaus, and D. Mayers, The European Physical Journal D **41**, 599 (2007).
- [18] S.-H. Sun, M. Gao, C.-Y. Li, and L.-M. Liang, Phys. Rev. A **87**, 052329 (2013).
- [19] C. C. W. Lim, M. Curty, N. Walenta, F. Xu, and H. Zbinden, Phys. Rev. A **89**, 022307 (2014).
- [20] S. Rahimi-Keshari, A. Scherer, A. Mann, A. T. Reza-khani, A. I. Lvovsky, and B. C. Sanders, New Journal of Physics **13**, 013006 (2011).
- [21] A. I. Lvovsky, H. Hansen, T. Aichele, O. Benson, J. Mlynek, and S. Schiller, Physical Review Letters **87**, 050402 (2001).
- [22] A. I. Lvovsky and M. G. Raymer, Reviews of Modern Physics **81**, 299 (2009).
- [23] A method for the calculation of the coefficients $P_\mu(k)$ directly from the experimental marginal distribution was proposed in: M. Munroe, D. Boggavarapu, M. E. Anderson, and M. G. Raymer, Phys. Rev. A **52**, R924 (1995).
- [24] C. Gerry and P. Knight, *Introductory quantum optics* (Cambridge university press, 2005).